Journal of Nuclear Materials 381 (2008) 185–198

Contents lists available at ScienceDirect

Journal of Nuclear Materials

journal homepage: www.elsevier.com/locate/jnucmat

# On estimating the fracture probability of nuclear graphite components

Makuteswara Srinivasan

*US Nuclear Regulatory Commission, Washington, DC 20555-0001, United States*

A B S T R A C T

The properties of nuclear grade graphites exhibit anisotropy and could vary considerably within a manufactured block. Graphite strength is affected by the direction of alignment of the constituent coke particles, which is dictated by the forming method, coke particle size, and the size, shape, and orientation distribution of pores in the structure. In this paper, a Weibull failure probability analysis for components is presented using the American Society of Testing Materials strength specification for nuclear grade graphites for core components in advanced high-temperature gas-cooled reactors. The risk of rupture (probability of fracture) and survival probability (reliability) of large graphite blocks are calculated for varying and discrete values of service tensile stresses. The limitations in these calculations are discussed from considerations of actual reactor environmental conditions that could potentially degrade the specification properties because of damage due to complex interactions between irradiation, temperature, stress, and variability in reactor operation.

Published by Elsevier B.V.

## 1. Introduction

It is well recognized that nuclear graphites have unique high-temperature capabilities, unlike any other material. Graphite processing involves typical ceramic processing steps. These include sizing, mixing, and blending of relatively high purity raw materials (coke particles and coke flour) with binder (e.g., petroleum or coal tar pitch), shaping the article by extrusion through a die or uniaxial compaction or isopressing, controlled-atmosphere baking to remove the binders and then pitch impregnation to fill the voids left by the escaping binders, re-baking and re-impregnation steps to improve the density and decrease the void content and to improve microstructural uniformity, and then final heat treatment in a controlled environment at a temperature in excess of 2500 °C which graphitizes the coke grains, coke flour, and the pitch impregnant. After ensuring complete graphitization, as determined by electrical resistivity, the graphite blocks are cooled in a controlled manner to minimize the number of microcracks that inevitably form due to graphite structure formation and cool-down stresses arising from the differences in the thermal expansion values in the *c*- and *a*-axis of the graphite hexagonal unit cell. As can be appreciated, any and all of these process steps, even when performed in a well-established and controlled manner, can lead to some level of micro- and macro-inhomogeneity in the resulting microstructure.

As a result of processing, the manufactured graphite is a composite of discrete and individual microstructures consisting of a distribution of graphitized coke particles and porosity of varying size, shape, and orientation. The graphitized binder pitch areas may also have a variety of size and shape distributions. Because of this distributed microstructure some degree of non-homogeneity is inherent in graphite which, in turn, results in a distribution in the observed values of properties, particularly strength. Recent grades of nuclear graphites are manufactured to be as isotropic as possible using iso-molding processing (equal applied stress in all directions of the formed compact) and finer coke particles. It should be noted, however, the anisotropy ratio usually refers to the ratio of the coefficient of thermal expansion (CTE) of graphite in the two orthogonal directions with an assumption of transverse isotropy in the values. The ratio of strength in the two orthogonal directions need not necessarily be the same as that observed for the CTE.

The variability in strength of graphite is not an insurmountable issue for estimating the reliability of graphite components in a nuclear reactor. Statistical techniques are well-advanced for analyzing fracture probability for ceramics [1], including graphite [2,3]. Although one can estimate the probability of fracture from material test results, translation and scaling of such data to predict the probability of fracture of a component involve a need to understand the influence of the state of stress on the fracture strength of test coupons and components. Typically, the state of stress in a graphite test coupon is rather simple. In a uniaxial tension test, the applied stress, which is tensile, is the same along the gauge length and the cross section of the test coupon. In a flexural bend test, the applied load can result in varying tensile and compressive stresses depending upon the location with

*E-mail address:* makuteswara.srinivasan@nrc.gov

0022-3115/$ - see front matter Published by Elsevier B.V.
doi:10.1016/j.jnucmat.2008.07.029

respect to the depth of the specimen tested. In an expanded ring test, biaxial tensile stresses result across the radius of the specimen. Thus, the strength values obtained from different test configurations and tests do not provide a unique value. Additionally, because of the inherent inhomogeneity, strength value varies within a test population for the same test. Therefore, such variations have to be first reconciled before scaling such probability strength distributions to estimate the fracture probability distribution of a component. Generally, it is understood that larger components can be expected to fracture at much lower mean strength values of a population of test coupons because of the relative higher probability of the existence of a detrimental critical flaw that will cause fracture.

The Weibull parametric estimates of the strength distribution also provide detailed information regarding the survival probability or the reliability under stress. In this paper, we will provide an analysis of reliability of the nuclear grade graphites using the mechanical properties as specified in the ASTM specification D7219-05 [4]. The material specification properties from this ASTM specification used in this paper are given in Table 1. In this table, the nuclear graphite classes are characterized by the manufacturing methods shown in Table 2.

The high purity nuclear graphite refers to nuclear graphite whose Boron Equivalent content is less that 2 ppm. The low purity nuclear graphite refers to nuclear graphite whose Boron Equivalent content is greater than 2 ppm but less that 10 ppm. The isotropic nuclear graphite refers to nuclear graphite whose isotropy ratio based on the coefficient of thermal expansion is 1.00–1.10. This ASTM standard is rather ambiguous with respect to the strength designation. It is not clear if the recommended strengths are actually the minimum strengths of a test population in bend or tension tests, or the average strengths of a test population in bend or tension tests. In this paper, it is assumed that the recommended values are the average strengths. It is also assumed that the average strengths can be equated to mean strengths for the purpose of this paper without serious error in the estimations of probability of fracture.

**Table 1**
ASTM specification D7219-05 for several nuclear graphite grades

| Material | Tensile strength (WG), MPa (psi) | Flexural strength (WG), MPa (psi) | Weibull modulus (WG) |
|---|---|---|---|
| IIHP, IILP | 22 (3191) | 35 (5076) | 15 |
| INHP | 20 (2901) | 30 (4351) | 12 |
| INLP | 15 (2172) | 21 (3046) | 12 |
| EIHP, EILP, ENHP, ENLP | 15 (2172) | 21 (3046) | 8 |
| MIHP, MILP, MNHP, MNLP | 15 (2172) | 21 (3046) | 10 |

**Table 2**
Nuclear graphite designation in ASTM specification D7219-05

| Graphite designation | Manufacturing method and purity |
|---|---|
| IIHP | Isomolded, isotropic – high purity |
| IILP | Isomolded, isotropic – low purity |
| INHP | Isomolded, near-isotropic – high purity |
| INLP | Isomolded, near-isotropic – low purity |
| EIHP | Extruded, isotropic – high purity |
| EILP | Extruded, isotropic – low purity |
| ENHP | Extruded, near-isotropic – high purity |
| ENLP | Extruded, near-isotropic – low purity |
| MIHP | Molded, isotropic – high purity |
| MILP | Molded, isotropic – low purity |
| MNHP | Molded, near-isotropic – high purity |
| MNLP | Molded, near-isotropic – low purity |

## 2. Weibull analysis for estimating risk of fracture

In this study, the analyses of the average strength data were performed using well-established mathematical formulations that relate the average strength, to Weibull modulus, $m$, and Weibull characteristic strength, $\sigma_0$. The material reliability under presumed service stresses were estimated using risk of fracture relationship with the safety factor and Weibull modulus. Appropriate considerations were incorporated to analyze the surface- and volume-originated fractures considering the importance of the state of stress on failure-causing flaws in the reliability predictions.

With respect to the state of stress, it is important to realize that, unlike a tensile test in which the tensile stress is uniform across the cross section, bend tests have non-uniform tensile stress across the specimen depth, linearly varying between the maximum value at the tensile surface to a minimum null value at the neutral axis which is one-half the specimen depth. Thus, a loading factor, $k$, exists which depends on the Weibull modulus. The loading factor, $k$, is unity for a tension test and it is less than unity for all other test methods. This loading factor is also different for surface area of the specimen and volume of the specimen tested and whether or not the fracture initiated at the surface or within the volume of the specimen.

The ASTM Material Specification D7219-05 refers to other ASTM specifications for determining the properties mentioned in the specification. For flexural strength determination, ASTM D7210-05 specification refers to the ASTM C871 specification, which itself refers to ASTM C651 specification. In this ASTM C651 specification, flexural strength is determined by a four-point loading using a third-point loading configuration, in which the support span is one-third of the loading span in the test. For this test configuration, the loading factors [5] are provided in Table 3 and shown in Fig. 1. Loading factors for other test configurations are also available in the literature [6].

The incorporation of the loading factor in the Weibull analysis formulation allows the normalization of strength data obtained by different test methods and to reconcile with the possible differences in volumes and surface areas of the tested specimens between various types of tests. Thus, the calculated risk of rupture[1] is given by the expression

$$R = \int_V \left(\frac{\sigma}{\sigma_0}\right)^m \mathrm{d}V, \tag{1}$$

where $\sigma$ is the applied stress, $\sigma_0$ is the Weibull characteristic strength (strength value at 63.2% of the Weibull strength distribution), and $V$ is the stressed volume. For engineering application of interest, this can be integrated to the form

$$R = kV\left(\frac{\sigma}{\sigma_0}\right)^m \mathrm{d}V, \tag{2}$$

where $k$ is the loading factor, as mentioned previously. We assume a two-parameter Weibull distribution, with the third parameter, the

[1] Throughout this paper, rupture and fracture will be used synonymously and indicates the onset or the initiation of the fatal crack (flaw) for further propagation under continued loading. It is recognized, particularly for graphite, that, in addition to this major propagating crack, additional cracking in the form of crack branching, new cracks away from the main crack, and cracks that are at orientations not exactly perpendicular to the main crack may also form and propagate under continued constant and increasing loading.

**Table 3**
Loading factors for third-point loaded bend test

| | |
|---|---|
| Surface loading factor, $k_s$ | $k_s = \frac{m+3}{6(\lambda+1)(m+1)}\left(\frac{1}{m+1}\right) + \lambda$, where $\lambda = b/d$, where $b$ is the specimen width and $d$, the depth |
| Volume loading factor, $k_v$ | $k_v = \frac{m+3}{6(m+1)^2}$ |

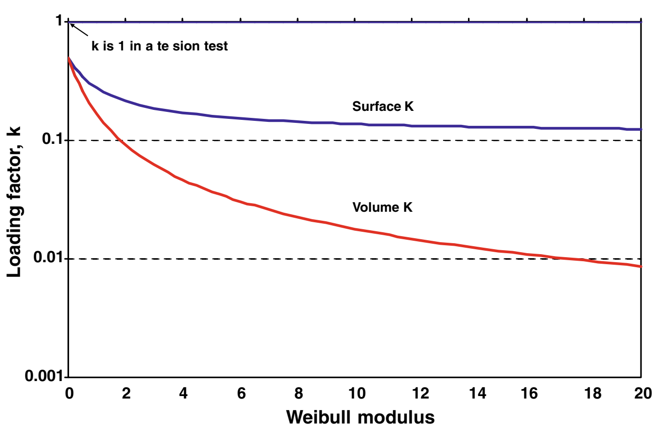


**Fig. 1.** The loading factors for strength tests mentioned in ASTM D7219-05.

minimum strength, $\sigma_u$, considered having a zero value. The Weibull probability of fracture expression can be expressed as

$$P = 1 - S = 1 - e^{-R}, \tag{3}$$

where $P$ is the probability of fracture (POF) and $S$ is the survival probability. The survival probability is also referred to as reliability.

From the strength distribution, the mean failure stress, $\sigma_m$, can be expressed as a gamma function of Weibull modulus as follows [7]:

$$\sigma_m = \sigma_0 \frac{\Gamma(1+\frac{1}{m})}{(kV)^m}. \tag{4}$$

From a combination of the above relationships, the quantity $kV$ can be eliminated to provide

$$S = e^{-\left[\frac{\sigma_s}{\sigma_m}\Gamma\left(1+\frac{1}{m}\right)\right]^m}. \tag{5}$$

Or,

$$S = e^{-R}, \tag{6}$$

where

$$R = \left[\beta\Gamma\left(1+\frac{1}{m}\right)\right]^m, \tag{7}$$

and

$$\beta = \frac{\sigma_s}{\sigma_m}. \tag{8}$$

Here $\sigma_s$ is the service stress corresponding to a given probability of survival. The reciprocal of $\beta$ is the material safety factor, $K_s$.

## 3. Analysis of ASTM material specification

The ASTM 651 standard does not provide exact dimensions of test specimen for 4-point bend test using third-point loading. However, guidance is provided that the size of the test specimen shall be selected such that the minimum dimension of the specimen is greater than 5 times the largest particle dimension. The test specimen shall have a length to thickness ratio of at least 8, and a width to thickness ratio not greater than 2. In this paper, an assumption is made that a width of 1.5 cm (0.590 in.) and a depth of 0.75 cm (0.295 in.) are used for the specimen with an inner (loading) span of 2.54 cm (1.000 in.) and an outer (support) span of 7.62 cm (3.000 in.). Thus, the volume of the specimen under tensile load is 4.29 $cm^3$ (0.260 $in^3$). This size for the test coupon is a reasonable assumption for the nuclear graphite classes mentioned in ASTM D7219-05 and may not deviate much from actual practice at various laboratories. Considering that, depending upon the size of the gas-cooled reactor, some graphite moderator blocks may be 1 meter cubes or approximately the same size of rectangular blocks, the volume of individual component block might be 1 $m^3$. Thus, the volume ratio of the component block to that of the specimen could be estimated to be approximately 233 320. Similarly, the total surface area exposed to tensile stress in the test specimen is 2.86 $cm^3$. The total surface area of the 1 $m^3$, if all these surface area experience tensile stress in service is 6 $m^2$. Thus the surface ratio of the component block to that of the specimen could be estimated to be approximately 10 500. These isovolumes[2] and isoareas are used in subsequent calculations in this paper in assessing the component properties scaled from test coupon.

The ASTM C 749 standard for tensile testing provides the dimensions for testing. The diameter of the test specimen is 0.953 cm (0.375 in.) and the gauge length, where the stress is uniform, is 1.905 cm (0.75 in.). In scaling up the size for the assumed 1 $m^3$ – size, the surface ratio of the component block to that of the specimen could be estimated to be approximately 10,525. The volume ratio of the component block to that of the tensile specimen could be estimated to be approximately 736 700.

A standard for size scaling methodology for advanced ceramics is being developed by ASTM Sub-committee C28.02 using tensile strength and Weibull statistics [8]. When fully developed, this standard may be used in the future to estimate the mechanical properties of component-size bricks of graphite from coupon test results.

Generally, because of machining and other surface stresses, and because the tensile stress is the maximum at the outer fiber of a flexural bend test, a majority of failures originate at the surface of the test specimen. However, this may not necessarily be true for an actual component in service. Based on the ASTM bend strength specification, the tensile strength was calculated using the following relationship:

$$\frac{\sigma_b}{\sigma_t} = \left(\frac{k_t}{k_b}\frac{A_t}{A_b}\right)^{1/m}, \tag{9}$$

where the subscripts for $\sigma$ refer to the mode of stress. The subscripts for $k$ (load factor) and $A$ (stressed area) refer to the type of test. The $k_t$ is unity. Using this calculated tensile strength, the risk of fracture for various levels of service stresses was calculated for various nuclear graphite classes for various stressed areas using the relationships shown in Eqs. (7) and (8). In addition, the risk of rupture was also calculated directly using the ASTM specification tensile strength data. For this calculation, the tensile strength of

[2] For rounding off purpose, a volume ratio of 250,000 is used in this study for properties scale-up and probability of fracture of components.

the test bar specification was scaled according to the surface area of the component using the following relationship

$$\frac{\sigma_t}{\sigma_c} = \left(\frac{1}{k_b}\frac{A_{tc}}{A_b}\right)^{1/m}. \tag{10}$$

In the above equation, $\sigma_t$ refers to the ASTM tensile strength specification and $\sigma_c$ refers to the calculated component strength, scaled-up from the equation. The factor $A_{tc}$ is the stressed area of the component and $A_b$ is the stressed area of the test bar. The factor $k_b$ is the surface load factor for the surface-flaws in the bend test.

In calculating the risk of fracture of the component based on the stressed volume, a similar scaling method was used for calculating the component strength from the ASTM specification strength using instead the volume load factor and the ratio of the stressed volumes.

## 4. Allowable service stress for assumed reliability in component design

The Westinghouse-proposed design practice [9] has modified and adapted the previously proposed, but not formally endorsed, German KTA rule for load categorization for ceramic structures, both in terms of quality class and in terms of types of loading category. Though not a consensus standard, a similar criterion was used [10] for the earlier German pebble-bed high-temperature reactor (HTR) [11]. The quality class definitions used in the modified-KTA rule are: The Class I components guarantee the stability of the core graphite structure, and hence guarantee its functioning. The neutron physics function is secondary. The Class II components perform primarily neutron physics function, namely moderation, reflection, and shielding. The mechanical function is secondary. The Class III components are for insulation and shielding. The mechanical function is secondary. The Westinghouse-proposed combination of quality assurance classes and the allowable fracture probabilities for loading categories (defined in Table 4) is shown in Table 5. Technical basis, experimental data, or other information on actual plant operational experience has not been provided to support the proposed classification. Apparently, this is the criterion that PBMR (Pvt) Ltd. will be using in their PBMR design [12].

A summary of previously used or recommended design criteria are provided below for comparison. Svalbonas et al. [13] previously suggested that the primary membrane and point stresses are not relevant as a special category in brittle materials. They also did not provide any suggestions for peak stresses and stated that these should be checked for creep-fatigue damage and/or by fracture mechanics methods. Their suggested allowable stress limits (fraction of the mean strength) for graphite components of the HTGR core are shown in Table 6. It was stated that the proposed limits were based on considerations of brittle design criteria, the safety orientation of the ASME code, and graphite behavior.

**Table 4**
Proposed loading categories for ceramic structures per Westinghouse report [9]

| Loading category (LC) | Event categorization |
|---|---|
| A | Normal operating conditions, anticipated abnormal occurrences, test cases, and incidents with a postulated incidence of $N > 1$ per plant design life |
| B | Hypothetical events, incidents with a postulated incidence of $N < 1$ per plant design life |

**Table 5**
Allowable failure probabilities (stresses) for combinations of loading category and quality class

| Quality class | Loading category A | Loading category B |
|---|---|---|
| I | 0.0001 | 0.001 |
| II | 0.0001–0.01[a] | 0.05 |
| III | 0.01 | 0.05 |

[a] The allowable fracture probability is 0.0001 at the beginning of service life and 0.01 at the end of service life.

**Table 6**
Suggested stress limits for graphite componentsof the HTGR core, Svalbonas et al. [13]

| Loading condition | Primary membrane stress | Primary point stress |
|---|---|---|
| Natural and upset | 0.25 | 0.33 |
| Emergency | 0.375 | 0.5 |
| Faulted | 0.53 | 0.7 |

**Table 7**
Proposed limit stress for general atomics prismatic design core, Alloway et al. [14]

| Fuel element type | Ratio of mean stress to mean strength |
|---|---|
| Stress group 1 | 0.35 |
| Stress group 2 | 0.31 |
| Stress group 3 | 0.26 |

Alloway et al. [14] have proposed the limits shown in Table 7 using probabilistic risk analysis techniques and claim that these allowable stress ratios will ensure that the plant investment and safety risk goals will be met. Thus, these stress limits seem to have been developed specifically for the General Atomics design of the HTGR. In the table, the group 1 refers to a small group of graphite core elements with an expected least probability of damage, the group 2 being those with the less and lower probability of damage in a larger group, and the group 3 elements having the higher probability of damage. Alloway et al. mentioned that the limit stress criteria for power production for control fuel element, replaceable reflector element, and for all components for shutdown, seismic, and accident conditions were under development.

The design criteria used for the graphite core and core support components for the Japanese high-temperature test reactor (HTTR) is very different from all of the above. The design criteria, though based on the ASME Sec. III, Div. 2, Subsection CE Code (draft), is substantially different and can be considered to be more rigorous. Two separate design stress limits were used for core support and core graphite components respectively; these stress limits were different for four categories of operations [15]. These are shown in Tables 8 and 9.

In these design limits, secondary stress limits have been specified conservatively in the same manner as the primary stress limits. Also, the peak stresses have been limited in order to prevent crack initiation and growth even under static fatigue conditions (possible crack extension under constant stress). The fatigue limits were claimed to be based on test data.

The exact definition of ‘minimum’ ultimate strength was not provided in Ref. [15]. It is noted that in the 3-parameter Weibull distribution of the strength data, the minimum strength has a particular meaning, that is, it is that strength below which the probability of fracture is zero. However, following traditional practice, the referred minimum strength could to be interpreted as the least acceptable minimum of the mean strength of the tested population.

The design of the Chinese HTR-10 used a modified-Japanese HTTR design approach [16]. The ‘minimum’ ultimate tensile strength was derived at 95% confidence and 99% reliability. The limiting stress was obtained from the ultimate strength using a safety factor of 3. Results of the computer calculations yielded

**Table 8**
Design stress limits for core graphite components for the Japanese HTTR (15)

| Operation Condition Category | Primary plus secondary stresses | | Peak stresses | |
|---|---|---|---|---|
| | Membrane $P_m$, $Q_m$ | Membrane plus bending or point Pb, Qb, Pp, Qp | Peak F | Fatigue |
| | $P_m + Q_m$ | $P_m + Q_m + P_b + Q_b$ or $P_p + Q_p$ | $P_m + Q_m + P_b + Q_b + F$ or $P_p + Q_p + F$ | |
| I & II | 0.33 $S_u$[1] | 0.5 $S_u$ | 0.9 $S_u$ | 1/3[2] |
| III | 0.5 $S_u$ | 0.75 $S_u$ | 0.9 $S_u$ | 2/3 |
| IV | 0.7 $S_u$ | 0.9 $S_u$ | 1.0 $S_u$ | 3/3 |

[1]$S_u$ is the specified minimum ultimate strength of the material.
[2]Allowable fatigue life usage fraction.

**Table 9**
Design stress limits for core support graphite components for the Japanese HTTR (14)

| Operation Condition Category | Primary plus secondary stresses | | Peak stresses | |
|---|---|---|---|---|
| | Membrane $P_m$, $Q_m$ | Membrane plus bending or point Pb, Qb, Pp, Qp | Peak F | Fatigue |
| | $P_m + Q_m$ | $P_m + Q_m + P_b + Q_b$ or $P_p + Q_p$ | $P_m + Q_m + P_b + Q_b + F$ or $P_p + Q_p + F$ | |
| I & II | 0.25 $S_u$[1] | 0.33 $S_u$ | 0.33 $S_u$ | 1/3[2] |
| III | 0.5 $S_u$ | 0.67 $S_u$ | 0.67 $S_u$ | 2/3 |
| IV | 0.6 $S_u$ | 0.8 $S_u$ | 0.8 $S_u$ | 3/3 |

[1]$S_u$ is the specified minimum ultimate strength of the material.
[2]Allowable fatigue life usage fraction.

values of 2.25 MPa (326 psi) for the membrane stress, 4.49 MPa (651 psi), for membrane plus bending stress, and 14.85 MPa (2153 psi) for the peak stress, which were all below the stress limits. For the graphite used in HTR-10, fracture probability during operation was estimated to be $2.3 \times 10^{-12}$, which increased to $4.7 \times 10^{-11}$ after cold shut down.

The AGRs of the UK have been designed with a different approach, based initially on a concept of 'reserve strength factor (RSF)' [17]. The mean strength of the graphite component, after taking into consideration the strength reducing effects of shrinkage and thermal stresses, known as the reserve strength, was compared with the stress generated by external loads in service. The RSF was defined as

$$\mathrm{RSF} = \frac{\text{irradiated strength-internal stress}}{\text{load applied stress}} \tag{11}$$

This factor was required to be greater than unity under reactor operating conditions. However, the statistical variability in the strength property of graphite made this approach not satisfactory to account for observed cracking of the bricks in service. Later, another criterion, called 'fractional remnant strength', $\Delta S$, was introduced which provided equal merits to various mechanisms of component failure, including the provision to include mechanisms that could be identified in the future. This was defined as

$$\Delta S = \frac{\text{shrinkage stress}}{\text{critical shrinkage stress}} - \frac{\text{thermal stress}}{\text{critical thermal stress}} - \frac{\text{applied load}}{\text{critical applied load}} - \frac{?}{\text{critical?}} \tag{12}$$

where '?' represents as yet 'unknown' loading not accounted for in the design. The ratio of the service stress to the failure stress is integrated over all possible failure mechanisms and, when $\Delta S$ is zero, the component will fail. This formulation has been verified experimentally [17]. This type of analysis has been claimed to provide information on the ability of the whole core to perform its function, despite the presence of broken core graphite blocks.

The service stresses in gas-cooled reactors can arise due to a variety of loads, the combination of which should be considered

**Table 10**
Coolant, pressures, and temperatures of various HTGR designs

| Reactor Designation | Country | Coolant | Coolant pressure, MPa (psi) | Coolant temperature, in/out, °C (F) |
|---|---|---|---|---|
| Dragon | UK | Helium | 2 (290) | 350 (662)/750 (1382) |
| Peach bottom | USA | Helium | 2.25 (326) | 377 (711)/750 (1382) |
| AVR | Germany | Helium | 1.1 (160) | 270 (518)/950 (1742) |
| Ft. St. Vrain | USA | Helium | 4.8 (696) | 400 (752)/775 (1427) |
| THTR-300 | Germany | Helium | 4 (580)–5 (725) | 270 (518)/750 (1382) |
| HTTR | Japan | Helium | 4 (580) | 395 (743)/950 (1742) |
| HTR-10 | China | Helium | 7.0 (1015) | 250 (482)/750 (1382) |
| GT-MHR (proposed new design) | USA | Helium | 7.0 (1015) | 490 (914)/850 (1562) |
| GT-MHR (1970s design, never built) | USA | Helium | 8.9 (1291) | 323 (613)/550 (1022) |
| PBMR | South Africa | Helium | 9 (1305) | 490 (914)/900 (1652) |
| AGR | UK | $CO_2$ | 4.4 (638) | 335 (635)/635 (1175) |

in the design stresses. These are mechanical loading stresses including those due to the coolant gas pressure, dead-weight loads, such as the static load of graphite bricks on the top of one another, internal (residual) stresses that may not be annealed out, stresses at key ways and support corners, thermal stresses, irradiation-induced loads, and impact stresses due to the movement of pebbles in the pebble-bed reactor. Therefore, it is very design-dependent. Because of this and other reasons, such as the unique neutron heating characteristics of the graphite and the thermal-hydraulics of block-design, in general, there has been no universally-accepted design codes for the graphite-moderated, gas-cooled, high-temperature reactor. Thus, the reliability estimate has to be performed for each reactor design separately and independently, based on the properties of graphite used, the thermal-hydraulics data, and the allowable stress limits for the particular design.

It is recognized that the time-dependency of the various loads are usually not considered in the initial graphite component reliability estimations, which are obtained based on the non-irradiated graphite properties. The gas pressure of the helium coolant varies from among reactor designs, ranging from less than 1 to 10 MPa (145 to 1450 psi), as shown in Table 10. The service (tensile) stress imposed on graphite moderator and reflector blocks does not does not necessarily equate to gas pressure. The service stress is expected to be substantially lower than the maximum gas pressure. However, depending on the geometry and the gas flow, some regions may experience higher stresses due to gas impingement related to flow considerations in a particular geometry.

## 5. Consideration of surface-initiated fracture

The coolant gas pressure has been stated to be 9 MPa (1305 psi) in the current proposed design of the pebble-bed modular reactor from PBMR (Pvt) Ltd., South Africa. Assuming that no other stresses would be present, this amount of stress at the surface of the bricks will crack one or more bricks as per the modified KTA rule, with increasing probability of fracture as other imposed stresses add to this amount of gas pressure, as shown in Fig. 2. The probability of fracture is based on the calculated tensile strength of the test coupon from the ASTM flexural strength and Weibull modulus specification for isomolded, isotropic nuclear graphite class, shown in Table 1, and using the surface load factor. Here, the probability of fracture is shown for various amounts of stressed area ratio (iso-area ratio lines) as a function of tensile service stress, assuming that fracture initiates at the surface of the bricks. For the case of surface area ratio of 10500, corresponding to approximate scaling from test coupon data to a 1-m size component, these isomolded, isotropic graphite class materials do not meet the failure probability criteria for I-A and II-A quality-stress category at the beginning of reactor life at proposed coolant gas pressure of 9 MPa.

Indeed, the fracture probability data shown in Fig. 2 are for a single brick. For a core containing several hundreds of bricks, the data indicate that fracture of at least several bricks at the start of reactor life is a good possibility at the expected gas pressures at the surface of the bricks.

It may be argued that this type of analysis is highly conservative because, in reality, not all surface areas of a component may be subjected to the same maximum amount of stress [14]. For a rigorous application, finite element analysis of a component in question will yield the distribution of the tensile stresses on the surface area of the component. One would then apply the above principle to the exact surface area of the component under specific stress levels, determined by the finite element analysis, to estimate the risk of fracture of individual discrete elements and then integrate or sum the individual risk of fracture of all the elements. This result is expected to provide lower risk of fracture values than the results shown in Fig. 2.

In fact these principles have been applied in the past for the design, manufacture, and application of structural ceramic components for demanding applications in automotive components [18–20]. Also, researchers at the National Aeronautics Space Administration (NASA) in Cleveland, Ohio have produced computer software to perform this analysis in a rigorous manner [21]. The Weibull statistical analysis was used for the design of graphite components for earlier German advanced high-temperature gas-cooled HTGR nuclear reactors [11]. Other similar probabilistic stress analysis techniques were used for gas-cooled reactors of General Atomics-design with prismatic graphite core blocks [14]. The Japanese HTTR has used the Weibull analysis for reliability estimations [22].

In this exercise, instead of using finite element analysis for the exact stress configuration of the theoretical brick, the probability of fracture (POF) calculations were performed for three cases of continuous step-wise decreasing service stress from a maximum value: case (1) by 10% for the component divided into 10 equal area elements, case (2) by the square of the distance away from the maximum value in 10 equal area divisions, and case (3) by the square of the distance away from the maximum value in 1000 equal area divisions. The probabilities of failure for each of these elements were calculated and integrated for the entire component and the results are shown in Fig. 3. It is observed that the variation in the risk of fracture estimation is negligible for the two cases of 10 equal area elements considered in this example. This result is not surprising since the maximum stress can be expected to predominate and dictate the initiation of fracture regardless of the variation from this maximum stress. The discretized elements and the cumulative risk of fracture of the elements to provide the total risk of fracture for the entire stressed surface area provides a probability of fracture value that is approximately an order of magnitude less that that obtained when uniform stress is assumed for all the area stressed. However, when the total surface

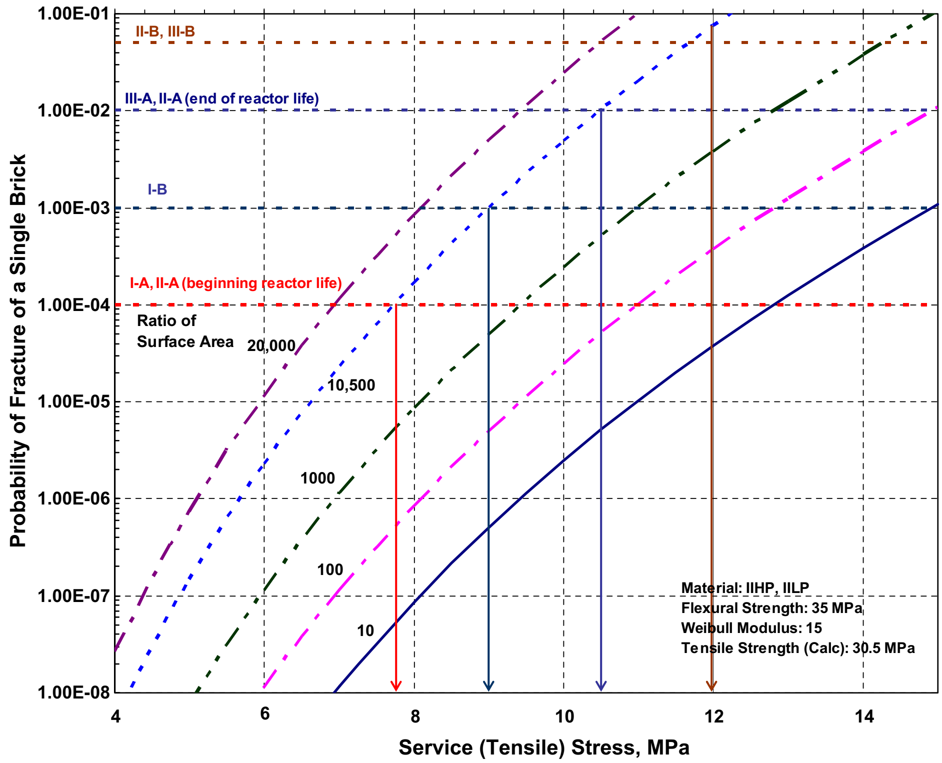


**Fig. 2.** The risk of fracture, based on ASTM specification for flexural strength and Weibull modulus for the isomolded, isotropic nuclear grade class, for varying tensile service stress and ratio of tensile surface area of component to that of the test specimen.

area is finely divided into 1000 equal surface area elements and the distribution of the stress is assumed to vary inversely with the square of the distance from the maximum stress location, the risk of fracture is at least two orders of magnitude less than that calculated for the total surface area experiencing the maximum service stress.

The implication of this result is significant in terms of meeting or not meeting the set failure criterion. For example, in scaling

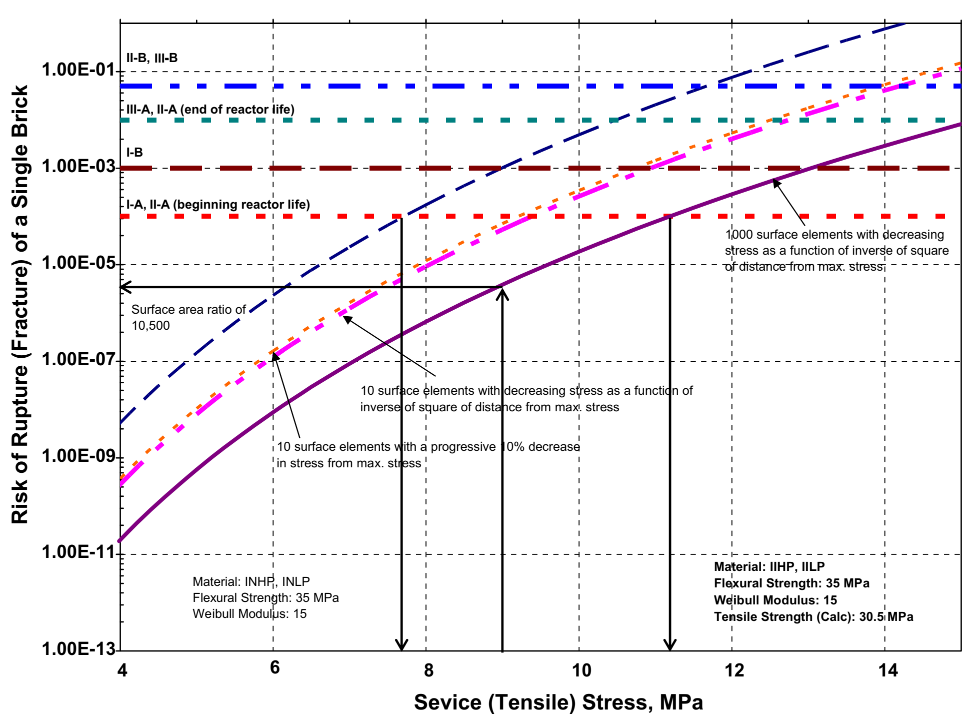


**Fig. 3.** The estimates of fracture probability, using a calculated tensile strength from ASTM bend strength specification for isomolded, isotropic graphite class, as a function of service stress for assumed stress variations within the stressed area of a graphite block.

from the test bar data to a hypothetical component, the probability of fracture for the entire component, assuming the stress distribution as above, is less than $1 \times 10^{-5}$ at a service stress of 9 MPa (1305 psi), where as the probability of fracture is approximately $1 \times 10^{-3}$ if the maximum stress acts on the entire surface area of the component. Conversely, in meeting the modified-KTA failure criterion of $1 \times 10^{-4}$ for the beginning of reactor life (criterion I-A), the maximum allowable service stress may be increased from less than 7 MPa to less than 11 MPa.

Although finite element analysis methods combined with risk of fracture analysis should be the preferred method and should be practiced in designing reactor components, this type of simple risk of fracture estimation can be performed to provide guidance on the probabilistic risk of fracture and the available safety margins for expected service stresses based on the probabilistic strength properties of nuclear graphite classes.

These calculations were continued using the tensile strength data given in the ASTM specification [4] but considered the scaling of the surface area from test specimen to the surface area component of the component on which the service stress is prevalent. The results of these calculations are shown in Fig. 4. Here, the tensile strength is approximately 28% less than that calculated from the flexural strength data for the same stressed volume or surface area. The effect on the estimated component probability of failure is striking. For the case of surface area ratio of 10500 between that of the assumed 1-m size component and the test coupon, at a service stress of 9 MPa, the estimated probability of failure of a single brick for the tensile strength estimated from the ASTM bend strength specification is 0.001, while it is 0.009 when estimated using the ASTM tensile strength specification. Thus, for fracture resulting from surface-flaws, using the ASTM tensile strength specification is more conservative than the ASTM bend strength specification in estimating the probability of failure of components from properties scaled-up from ASTM bend and tensile test data.

In Fig. 5, failure probability estimates for surface-flaw initiated fracture of the components are shown for various ratios of component-test coupon surface areas based on the ASTM tensile strength specification. The effect of the decreased reliability for the structural integrity of the component as the stressed area is increased is clear. Even considering one-half of the area of the typical component size considered in this paper, the risk of fracture is greater than the modified KTA-rule requirement of 0.0001 for I-A category for an assumed service stress of 9 MPa.

As previously discussed for the case of probability of fracture estimates using tensile strength calculated from bend strength specification, similar calculations were also performed using the tensile strength for assumed stress variation in the total area of the component. The results are shown in Fig. 6 for assumed variations in stress in the stressed area of the component for the ASTM specification isomolded, isotropic nuclear graphite class.

The results clearly show the effects of stressed surface area in influencing the onset of fracture of the component. From the results of the case of the total surface area divided into 10 units, significant difference in the probability of failure does not occur between the two cases of assumed stress variations. However, segmentation into larger number of areas of continuously decreasing stress from a maximum value does play a major role in enhancing the reliability of the component under assumed service stresses.

## 6. Consideration of fracture initiation in the interior of the component

Similar calculations were performed considering the volume of the stressed component and using the minimum bend and tensile strength requirements of ASTM specification D7219-05, respectively. The scaling calculations for the component were continued using the bend strength test data. Assuming that uniform stress is present in the entire volume of the block, the probability of fracture estimates are shown in Fig. 7 for various ratios of volume of the block to the test specimen. Applying previous discussions, it appears that components of typical sizes can be expected to have the initiation of fracture under PBMR normal operational conditions with imposed stresses of greater than 5 MPa (725 psi) for the proposed quality-stress category acceptance criteria.

As discussed before, the reliability, under realistic conditions of stress distribution will probably be much higher for the components

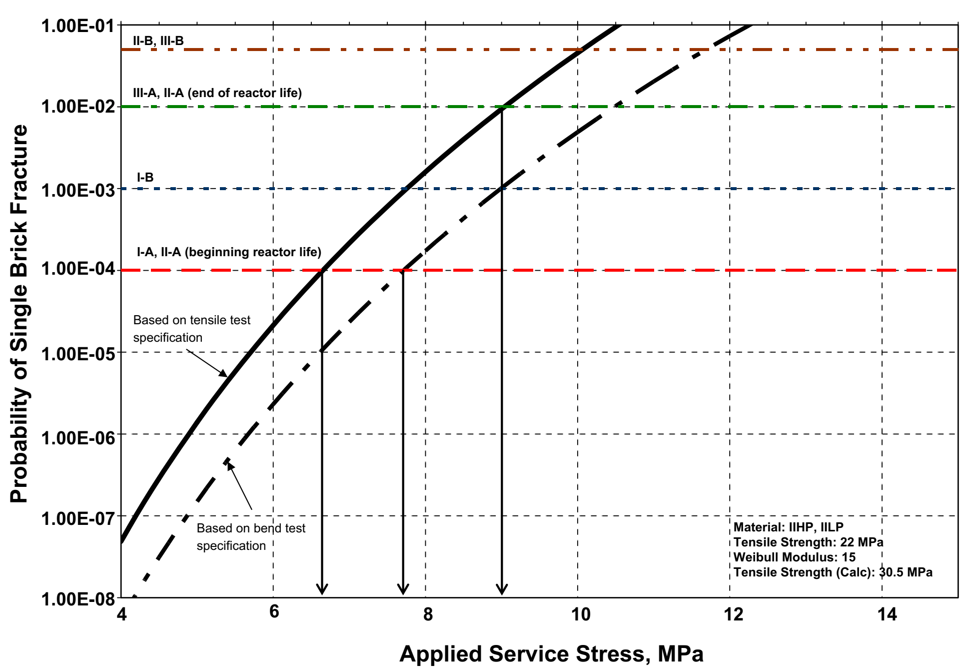


**Fig. 4.** Effect of differing tensile strengths of isomolded, isotropic graphite class in ASTM specification between that calculated from bend strength and specification tensile strength on the estimated probability of failure.

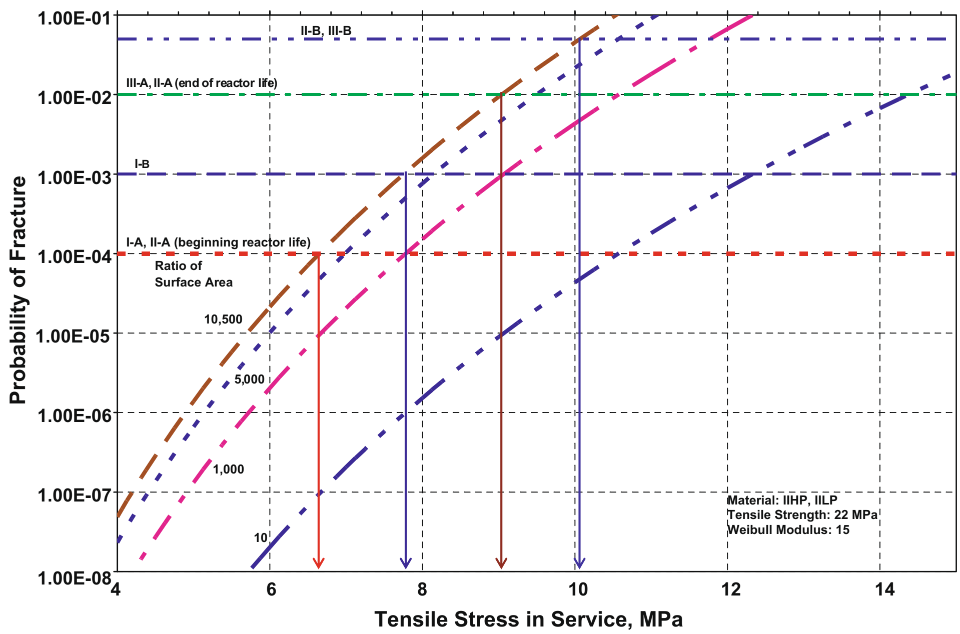


**Fig. 5.** The risk of fracture, based on tensile strength and Weibull modulus, for isomolded, isotropic nuclear grade classes of ASTM specification for varying tensile service stress and ratio of tensile surface area of component to that of the test specimen.

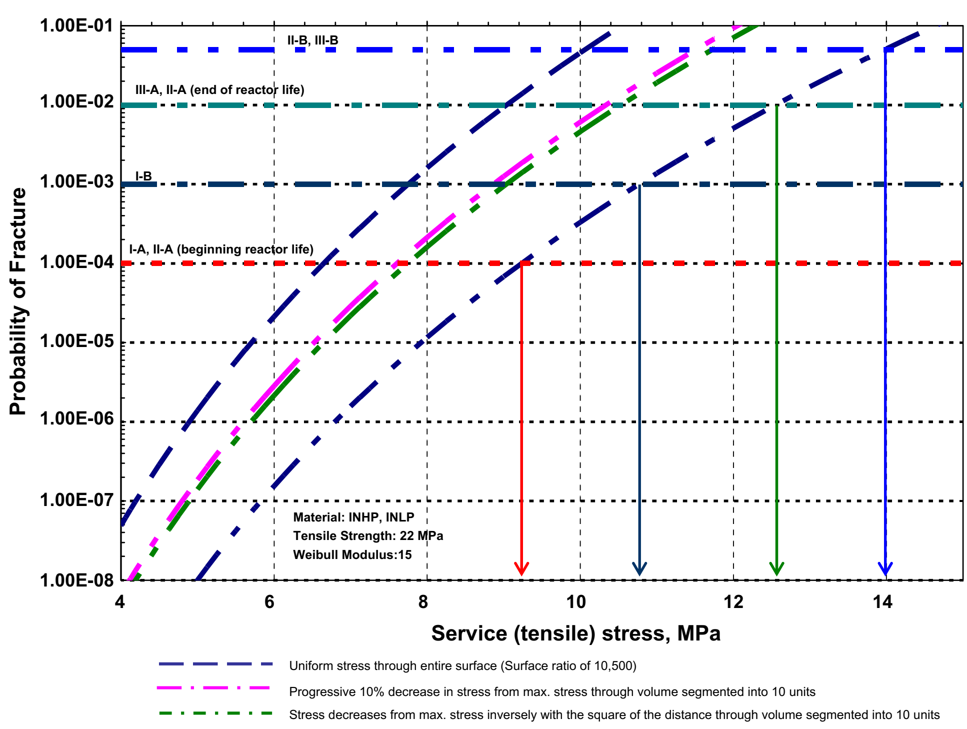


**Fig. 6.** The estimates of fracture probability, using ASTM tensile strength specification, as a function of service stress for assumed stress variations within the stressed area of a graphite block.

because the maximum stress probably will act only on some limited volume of the component. A simulation of such distributed stress condition was conducted under the same assumed conditions used for the calculation for stressed area, mentioned previously. Thus, three cases were analyzed in which the maximum service stress was decreased step-wise and continuously by three different approaches: (a) 10% for volume elements divided into 10 equal elements; (b) the square of the distance away from the maximum value in 10 equally divided volume elements, and (c) the square of the distance away from the maximum value in 1000 equally divided volume elements. The results are shown in Fig. 8. We observe that even under the most favorable stress distribution condition and volume segmentation, the estimated fracture probability is at least an order of magnitude greater than the

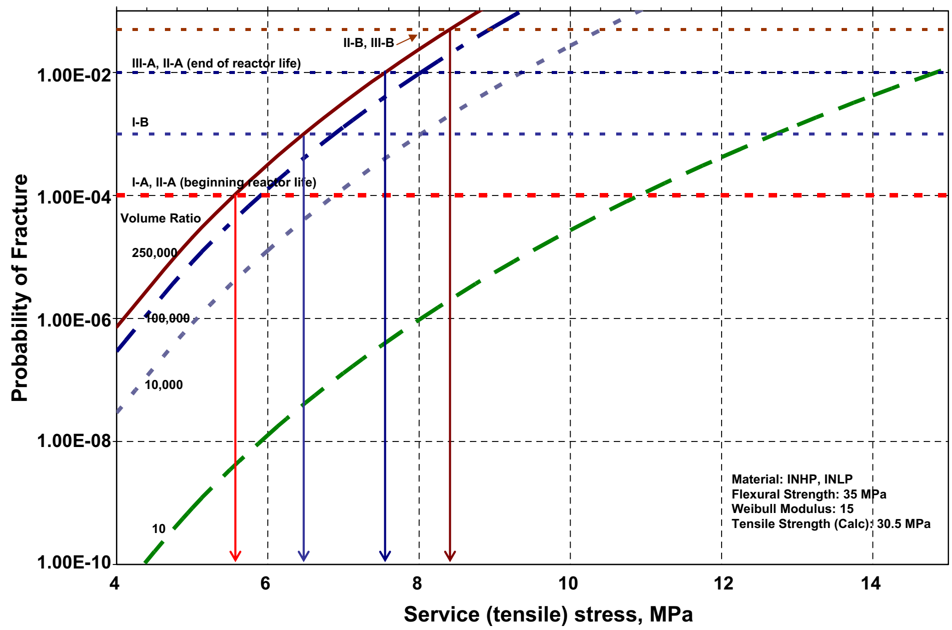


**Fig. 7.** Estimates of fracture probability for various volume ratios of component to test coupon, based on bend strength and Weibull modulus for the isomolded, isotropic ASTM specification graphite class.

modified-KTA rule requirement for I-A conditions at an assumed helium coolant gas pressure of 9 MPa.

## 7. Reliability of other ASTM Specification graphite classes

Similar calculations can be performed for other graphite classes in the ASTM specification. For the case of isomolded, near-isotropic graphite class, the estimated probability of fracture of a single brick, from surface-flaws and from flaws in the volume of the brick, is shown for tensile strength derived from bend data and the actual minimum tensile strength ASTM specification in Fig. 9. It is seen that the probability of fracture, as expected, is a strong function of the origin of fracture and is influenced by the tensile strength of the block scaled from the test coupon data. The most conservative estimate of failure of the probability of fracture is obtained using the ASTM tensile

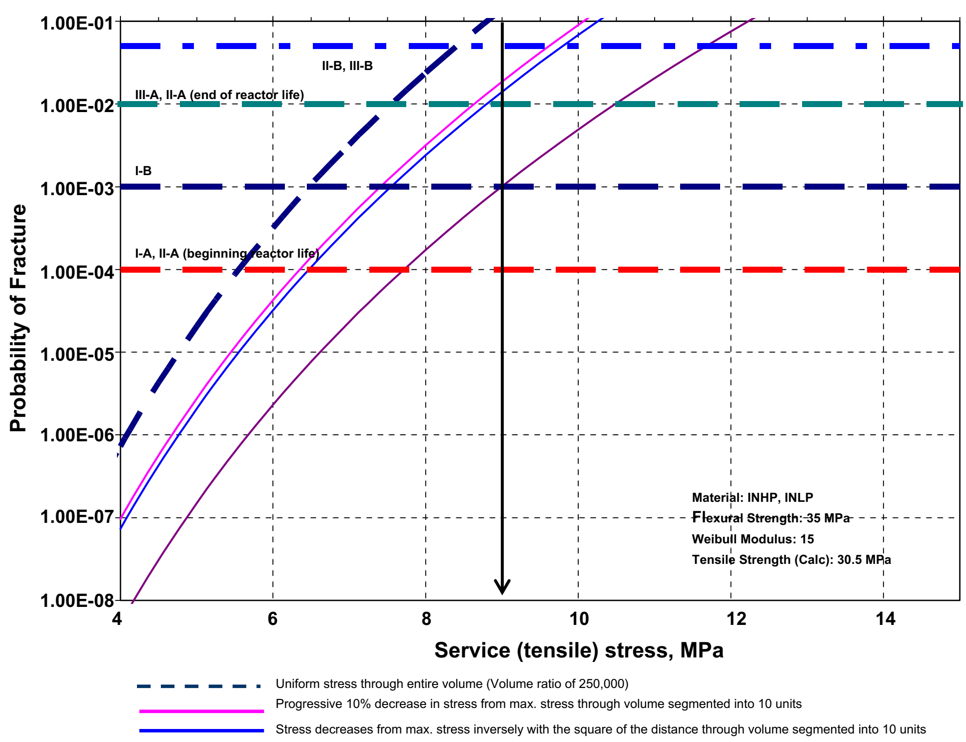


**Fig. 8.** The estimates of fracture probability, using ASTM tensile strength specification, as a function of service stress for assumed stress variations within the stressed volume of a graphite block.

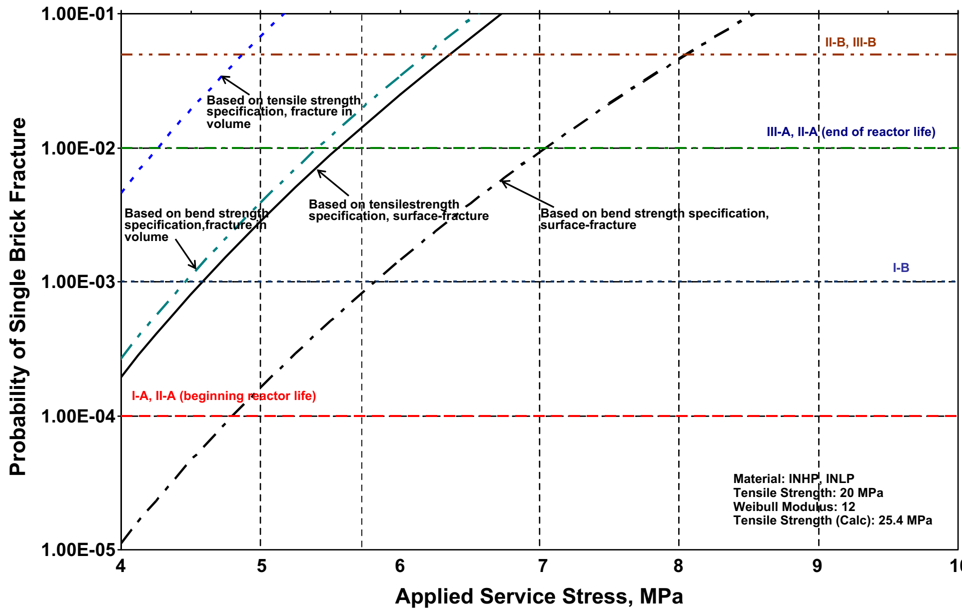


**Fig. 9.** Effect of differing tensile strengths of isomolded, near-isotropic graphite class in ASTM specification between that calculated from bend strength and specification tensile strength on the estimated probability of failure assuming fracture origin at the surface or in the interior of the brick.

strength specification and assuming the failure origin in the interior of the block.

A significant implication of this result is a required assurance of minimum quality for the interior of the block. Although qualitative and quantitative surface examination and the establishment of acceptable quality levels are possible, it is not presently clear that such assurances are possible for the absence of interior flaws in component-sized graphites. Another implication of these results is the importance of obtaining reliable mechanical properties data from samples irradiated in representative environments of the reactor design. In designing specimens, testing procedures and analyzing test results, considerations must be given on how the irradiated properties data from test specimens will be used to predict the irradiated properties of actual components and the size effects which have been considered here.

For the other ASTM specification classes, mainly because of the lower values of tensile strength, the probability of fracture of graphite bricks are substantially higher than that for the isomolded, isotropic class graphite, when the brick properties are scaled from the specification properties considering the surface area and the volume effect. The results are shown in Figs. 10 and 11 for the failures originating at the surface and in the interior of the brick. At substantially less than the proposed gas pressures of 9 MPa (1305 psi) in the PBMR, fracture in bricks made from these nuclear graphite classes can be expected for the modified-KTA rules for acceptable fracture limits, based on ASTM specifications.

## 8. Uncertainties in the probability of failure estimate

Several sources of uncertainties exist in the analysis presented in this study; these uncertainties will also apply to finite element analysis based stress calculations and estimates of probability of failure. Among these, two are particularly relevant. The first is the model uncertainty. The calculation of tensile strength from the bend strength and Weibull modulus depends upon the unique equivalence in the tensile strength calculated by this procedure and the actual tensile strength of the material. As we have seen in this example, the tensile strength calculated by the ASTM bend strength and the Weibull modulus specification differs considerably from the ASTM tensile strength specification. The difference could arise from the microstructure difference in the test population of the respective tests. Such uncertainty can further exacerbate the probability of fracture estimate of a large graphite brick estimated from the Weibull-type statistical scaling procedure.

A second uncertainty in the prediction could result from the data uncertainty. Several elements can contribute to the data uncertainty. First, because even isomolded classes of nuclear graphite can exhibit limited non-homogenous microstructure within a large block, the test sample data, from which properties of the large block can be estimated, should be representative of the area (volume) of the block for which the tensile strength property will be used for estimating the probability of failure for that respective area (volume) of the block. If not, considerable error in the estimate could arise. Second, the strength of graphite can be expected to be a function of the surface condition, especially for the population for which the strength is largely determined by the presence of surface-flaws. In this case, in order to extrapolate the data from test coupon to component, it should be ensured that the surface condition is the same for both, namely machining and polishing. To avoid edge-originating failures, it is customary to chamfer the edges of bend test bars. The edges of the components should also be similarly chamfered for appropriate extrapolation of the test bar data. Third, there exists data uncertainty in the results of the bend or tensile tests conducted to confirm the ASTM specification properties. The bend and tensile test results yield average strength, a characteristic strength, and a Weibull modulus. Of these, it is well known that the Weibull modulus is a strong function of the number of samples tested. It has been shown that a minimum sample population in the range of 110–120 is required for convergence in Weibull modulus. This requirement impacts the estimation of failure probability significantly. Even when 120 samples are tested, the lowest data point for probability of failure is $8.26 \times 10^{-3}$. To obtain an experimental value for demonstration of required probability of fracture of $1 \times 10^{-4}$, one needs to test 10000 specimens, which is not realistic. The consequence is that, when one generates 95% confidence bands for experimental data, there is large divergence in the probability of failure at very low stress values of the tested population. The uncertainty due to the lack of adequate sampling could contribute to significant error in the estimation of the probability of fracture at low probability

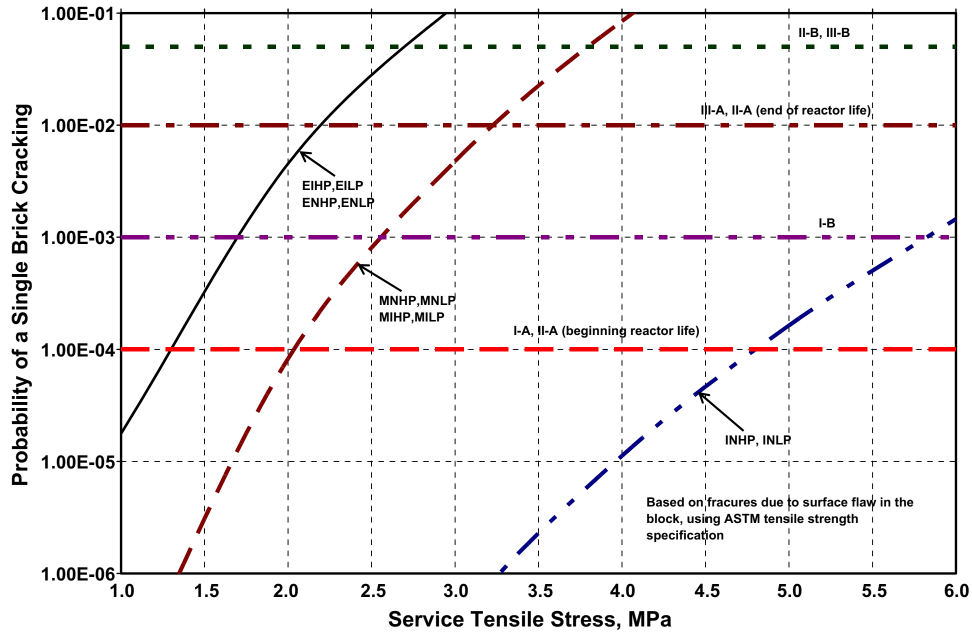


**Fig. 10.** Probability of fracture of ASTM specification nuclear graphite classes based on failure from surface-flaws.

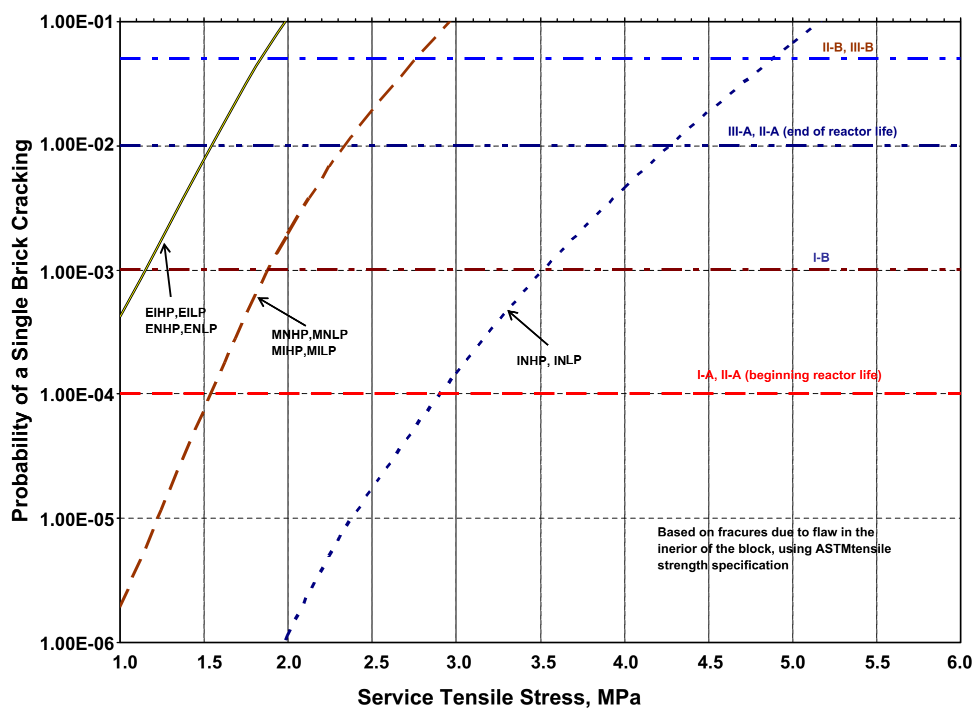


**Fig. 11.** Probability of fracture of ASTM specification nuclear graphite classes based on failure from interior flaws.

of failure for both test bar specimens and for large components [23].

When the number of tested population is less than 25, the estimated failure probability of different batches of a nominally the same material can vary by more than several orders of magnitude. For example, when only five specimens are tested per condition, the actual probability of failure can be as high as 0.13, when the extrapolated (predicted) level is 0.0001. Although this result corresponds to a worst case, other results indicated that the upper limit is often about 0.013, which would not be acceptable in any engineering application, let alone in a nuclear application. When the test population is increased to 25, the highest upper limit in the confidence interval was about 0.0003, which is only 3 times the desired probability of 0.0001 [23].

## 9. Limitations

There are several other limitations to this procedure for estimating the probability of failure of the component from limited data from test coupons. Some of these limitations are explained below:

1. An obvious major limitation is the lack of adequate representation of the exact reactor environment for the coupon tests. The ASTM mechanical properties specification are for data obtained from room temperature tests conducted in ambient air. Thus, any estimate of failure probability of the component from these data is only applicable to the test conditions of the specification. Changes in properties with the environmental condition in the reactor should be modeled and appropriately considered in estimating the failure probability of components in service, which can consequently change with time. These data are essential to establish the potential degradation of available service margin over reactor operation.
   a. Generally, graphite strength increases with both temperature and irradiation; however, other physical and thermal properties change in a complex manner. Thus, these estimations are not applicable during service or at the end of service life. The time and dose-dependent properties are needed to perform such estimations of the time-dependent probabilities of failure to ascertain whether or not the failure criteria II and III of the modified-KTA rule will be met, and to estimate the time-dependency of safety margin of graphite core components during plant operation.
   b. Properties of graphite could be adversely affected by impure helium coolant and the presence of an oxidative environment [15,24]. It is also expected that graphite dust will be a constituent of the coolant. Both oxidation and potential erosion of the graphite block by graphite dust can significantly degrade the surface-structure of the graphite component. The effect of such surface degradation on the strength and fracture toughness [25–27] is an important consideration in extrapolating the properties of test bars to component behavior in a reactor.
   c. The effects of cyclic [28] and static fatigue [29] in reducing the allowable operational stress should be incorporated in a thorough analysis. Time-dependent property changes influence the behavior of graphite to a significant extent and therefore should be properly considered for a rigorous analysis of the life of the graphite component. Even though these data may not be available for the timely design and new reactor commissioning, to assure safety in the absence of an established, verified and validated failure theory [30], the design should be sufficiently conservative so that the service stresses are kept remote from the accepted probability of failure criteria [13].
   d. Graphite is unlike any other material typically used in a nuclear reactor. The major property of concern is the dimensional change of graphite under irradiation. Typically, during early operational years it shrinks in volume under low doses and then in later years of operation, after considerable neutron damage, the magnitude of shrinkage decreases continuously (what is known as 'turnaround'). The time (dose) at which this turnaround occurs is usually defined as the useful life for graphite [31]. Beyond the turnaround, the contraction stops and eventually the graphite begins to expand with increased dose or reactor operation. A significant contributor to this behavior is the creep of graphite under irradiation, much like the thermal creep under stress for metallic materials [32]. The fracture of graphite during reactor operation is thus governed by these complex interactions that contribute to strain accommodation during reactor service. These complex features can be analyzed for particular designs to estimate graphite life [17]. This feature can not be duplicated readily in the probability of fracture calculations based on simple mechanical properties, such as strength and the strength distribution, represented by Weibull modulus.
   e. The strength distribution, as represented by Weibull modulus, is used in the failure probability estimations. The possible dependence of Weibull modulus on irradiation dose, temperature, and time should be established for rigorous estimations.
2. The stress at the root of notches and other areas where graphite bricks come in contact with other bricks and/or connecting dowels will be much higher than the stress in the bulk graphites due to the stress concentration effect [31]. Thus, the strength used for probability of failure predictions cannot be used as such for fracture originating at the notches and other areas of potential stress intensification.
3. The ASTM specification mentions only the properties measured along the grain orientation, which is probably sufficient for isotropic class of nuclear graphite. For other than this type graphite, the properties measured in the direction normal to the grain (against-grain orientation) are expected to be less than those measured in the with-grain direction. Thus, the strength values used are not conservative for those graphites other than the isotropic class. Likewise, the extrapolation of POF estimates is also not conservative.
4. The rate of loading is an important operational variable that has not been considered in this simple analysis. Data on graphite strength as a function of loading rate (strain rate) and temperature are needed to incorporate these effects in the fracture prediction models. Especially during transients, these effects could be significant.
5. The initiation of cracks and their limited propagation in graphite component may not necessarily result in the failure of the component to adequately perform its intended function, structural, moderator and reflector of neutrons, and shielding. In fact, it is well known that in spite of the presence of several cracks and their, perhaps, limited propagation, in many of the UK's AGRs [33,34] and in Russian gas-cooled reactors [35], these reactors have functioned safely to produce power. One of the functional requirements of graphite blocks containing fuel rod channels and control rod channels is the ability to maintain sufficient clearance to allow free and easy movement of fuel rods and control rods. If the initiation and propagation of cracks do not distort the geometry of the component to adversely affect the fuel rod and control rod movements, the functionality of graphite still may be adequately maintained. However, the 'tolerability' of such fracture, the 'tolerability' of the presence of multiple cracks within a single block, and the 'tolerability' of the presence of a number of graphite blocks with single and multiple cracks in ensuring adequate geometry for safety need to be demonstrated for specific reactor design. Such demonstration is not expected to be easy or straight forward, because of the dimensional changes and the changes in the properties affecting crack initiation and crack propagation.

## 10. Summary and conclusions

The probability of fracture of typical nuclear graphite component was estimated based on recently published ASTM mechanical properties specifications. Well-established Weibull statistical estimation procedures were applied in scaling the properties from the specification properties to those of a typical component, assuming fracture to initiate at the surface and in the interior of the component respectively. These calculations indicate that the current ASTM nuclear graphite specifications may not be adequate to meet the required reliability proposed in the modified-KTA design rule.

The limitations in this simple approach have been outlined in this paper; however, proper considerations of these limitations may still result in most of the graphites not meeting the proposed minimum reliability under reactor environment.

The results of this study have indicated the relative importance of proper design of test specimen configuration, test method, and the analysis of mechanical properties test data for extrapolation and scaling to estimate the expected performance of actual components in reactor service.

## Acknowledgements

The author appreciates the valuable review of this paper by several NRC staff members.

## References

[1] A. Palusny, W. Wu, J. Eng. Power, Trans. ASME, Paper No. 77-GT-41, 1977.
[2] H. Cords, G. Kleist, R. Zimmermann, in: IAEA Specialists Meeting on Mechanical Behaviour of Graphite for High Temperature Reactors, Gif-sur-Yvette, France, 11–13 June 1979.
[3] R.C.B. Judge, in: Proceedings of IAEA Specialists Meeting on Graphite Component Structural Design, Tokai Mura, Japan, 1991, p. 78.
[4] ASTM D 7219-05, Standard specification for isotropic and near-isotropic nuclear graphites, American Society for testing Materials, 2005.
[5] N.A. Weil, I.M. Daniel, J. Amer. Ceram. Soc. 47 (6) (1964) 268.
[6] S.G. Seshadri, M. Srinivasan, J. Mater. Sci. 16 (1981) 3052.
[7] G.J. DeSalvo, Theory and structural design applications of Weibull statistics, Westinghouse Electric Corporation Astronuclear Laboratory Report, WANL-TME-2688, 1970.
[8] Size scaling of tensile strengths using Weibull statistics for advanced ceramics, ASTM Proposed Standard Practice, Under Preparation, Personal communication, S.F. Duffy to M. Srinivasan, 2006.
[9] Regulation for the design of the internals of the high temperature reactor, Version May 2003, Westinghouse Preliminary Report, Document No. GBRA 065 942, 2003.
[10] H. Nickel, F. Schubert, H. Breitling, E. Bodmann, Nucl. Eng. Design 121 (1990) 183.
[11] E. Bodmann, in: Proceedings of IAEA Specialists meeting on Graphite Component Structural Design, JAERI, Tokai, Japan, Paper I-3, JAERI-M 86-192, 8–11 September 1986.
[12] Technical Description of the PBMR Demonstration Power Plant, Revision 4, Document No. 016956, PBMR (Pvt) Ltd., NRC document, ADAMS No. ML060940293, 2006.
[13] V. Svalbonas, T.C. Stilwell, Z. Zudas, Nucl. Eng. Design 46 (1978) 313.
[14] R. Alloway, W. Gerholt, F. Ho, H. Vollman, H. Yu, in: Proceedings of IAEA Specialists Meeting on Graphite Component Structural Design, Tokai Mura, Japan, 1986.
[15] T. Ioyoku, S. Shiozawa, M. Ishihara, T. Arai, T. Oku, Nucl. Eng. Design 132 (1991) 23.
[16] Z. Zhensheng, Yu. Suyuan, Z. Zhengming, Presented at the Review of UK and Chinese Methodologies for Assessing Graphite Stresses in Nuclear Graphite Component, University of Manchester, UK, 2–3 October 2002.
[17] N. McLachlan, R.T. Szczepura, M.A. Davies, R.C.B. Judge, B.J. Marsden, Nucl. Energy 35 (1) (1996) 15.
[18] D.G.S. Davies, Proc. Brit. Ceram. Soc. 22 (1973) 429.
[19] A. Palusny, W. Wu, J. Eng. Power, Trans. ASME, Paper No. 77-GT-41, 1977.
[20] M. Srinivasan, S.G. Seshadri, in: Proceedings of ASME Failure Prevention and Reliability Conference, Hartford, CT, USA, 10–23 September, 1981.
[21] N.N. Nemeth, L.M. Powers, L.A. Janosik, J.P. Gyekenyesi, Time-dependent reliability analysis of monolithic ceramic components using the CARES/LIFE integrated design program, in: C.R. Brinkman, S.F. Duffy (Eds.), Life Prediction Methodologies and Data for Ceramic Materials ASTM STP 1201, American society for Testing and Materials, Philadelphia, 1993, p. 390.
[22] M. Ishihara, H. Mogi, I. Ioka, T. Arai, T. Oku, in: IAEA Specialists meeting on Graphite Component Structural Design, JAERI, Tokai, Japan, Paper I-7, JAERI-M 86-192, 8–11 September 1986.
[23] S.G. Seshadri, M. Srinivasan, J. Eng. Mater. Technol. Trans. ASME 105 (1983) 220.
[24] T. Maruyama, in: Proceedings of IAEA Specialists meeting on Graphite Component Structural Design, JAERI, Tokai, Japan, Paper I-3, JAERI-M 86-192, 8–11 September 1986.
[25] S. Sato, K. Hirakawa, A. Kurumada, S. Kimura, E. Yasuda, Nucl. Eng. Design 118 (1990) 227.
[26] D.G. Schweitzer, Experimental results of air ingress in heated graphite channels: A summary of American analysis of the Windscale and Chernobyl accidents, IAEA-TECDOC-784, 1995.
[27] W. Katscher, R. Moormann, K. Verfondern, C.B.v.d. Decken, A. Christ, G. Lohnert, U. Wawrzik, Nucl. Eng. Design 121 (1990) 219.
[28] M. Futakawa, Y. Kikuchi, Y. Muto, H. Shibata, in: Proceedings of IAEA Specialists meeting on Graphite Component Structural Design, JAERI, Tokai, Japan, Paper I-3, JAERI-M 86-192, 8–11 September 1986, p. 87.
[29] B.J.S. Wilkins, J. Am. Ceram. Soc. 54 (12) (1971) 593.
[30] S. Aoki, L. Ohta, H. Ohnabe, M. Sakata, Int. J. Fract. 21 (1983) 285.
[31] N. Prince, J.E. Brocklehurst, in: Proceedings of IAEA Specialists meeting on Graphite Component Structural Design, JAERI, Tokai, Japan, Paper I-3, JAERI-M 86-192, 8–11 September 1986.
[32] B.C. Mitchell, B.J. Marsden, J. Smart, S.L. Fok, Nucl. Energy 40 (2001) 1.
[33] J. Reed, Presentation at the Sixth International Nuclear Graphite Specialists Meeting (INGSM-6), Chamonix, France, September 2005.
[34] J. Reed, Presentation at the Ageing Management of Graphite Cores Conference, University of Cardiff, November, 2005.
[35] P.A. Platanov, O.K. Chugunov, V.N. Manevsky, V.I. Karpukhin, in: Proceedings of a specialists meeting held in Bath, UK, 24–27 September 1995, IAEA-TECDOC-901, 1996, p. 79.